Nat. Hazards Earth Syst. Sci., 17, 115–125, 2017
www.nat-hazards-earth-syst-sci.net/17/115/2017/
doi:10.5194/nhess-17-115-2017

Natural Hazards and Earth System Sciences
Open Access
EGU

Heat waves in Africa 1981–2015, observations and reanalysis

Guido Ceccherini[1], Simone Russo[2], Iban Ameztoy[1], Andrea Francesco Marchese[3], and Cesar Carmona-Moreno[1]

[1]European Commission, Joint Research Centre (JRC), Directorate D – Sustainable Resources, Water and Marine Resources, Via E. Fermi 2749, 21027 Ispra (VA), Italy
[2]European Commission, Joint Research Centre (JRC), Directorate I – Modelling, Indicators and Impact Evaluation Unit, Via E. Fermi 2749, 21027 Ispra (VA), Italy
[3]Università degli Studi di Catania Dipartimento di Fisica e Astronomia, Via Santa Sofia 64, 95123 Catania, Italy

Correspondence to: Guido Ceccherini (guido.ceccherini@ext.jrc.ec.europa.eu)

Received: 18 March 2016 – Published in Nat. Hazards Earth Syst. Sci. Discuss.: 18 April 2016
Revised: 5 January 2017 – Accepted: 11 January 2017 – Published: 30 January 2017

Abstract. The purpose of this article is to show the extreme temperature regime of heat waves across Africa over recent years (1981–2015). Heat waves have been quantified using the Heat Wave Magnitude Index daily (HWMId), which merges the duration and the intensity of extreme temperature events into a single numerical index. The HWMId enables a comparison between heat waves with different timing and location, and it has been applied to maximum and minimum temperature records. The time series used in this study have been derived from (1) observations from the Global Summary of the Day (GSOD) and (2) reanalysis data from ERA-Interim. The analysis shows an increasing number of heat waves of both maxima and minima temperatures in the last decades. Results from heat wave analysis of maximum temperature ($HWMId_{tx}$) indicate an increase in intensity and frequency of extreme events. Specifically, from 1996 onwards it is possible to observe $HWMId_{tx}$ spread with the maximum presence during 2006–2015. Between 2006 and 2015 the frequency (spatial coverage) of extreme heat waves had increased to 24.5 observations per year (60.1 % of land cover), as compared to 12.3 per year (37.3 % of land area) in the period from 1981 to 2005 for GSOD stations (reanalysis).

1 Introduction

Africa is considered one of the most vulnerable regions to weather and climate variability (Solomon, 2007); extreme events such as heat waves have an impact to public health, water supplies, food security. According to Albrecht (2014), climate change will increase its pressure in northern Africa. All African capital cities are anticipated to face more exceptionally hot days in the future with respect to the rest of the world.

In fact, recent findings of the World Meteorological Organization (WMO) indicate that the years 2011–2015 have constituted the warmest 5-year period on record (WMO, 2015) and heat waves of maximum temperature have increased both in severity and number accordingly.

Despite its vulnerability, the distribution of African heat waves is still poorly understood due to the lack of accurate baseline data on current climate (UNECA, 2011). Specifically there are still uncertainties in the state of the art of our actual understanding of temperature extreme regime; only a few studies have considered the whole of Africa (Collins, 2011). Such information is paramount, since it is necessary to assess the impacts of climate change on human and natural systems and to develop suitable adaptation and mitigation strategies at country level.

Daily records are needed in order to analyse extreme temperature regimes. To this end, the Global Surface Summary of the Day (GSOD) meteorological dataset has been employed. GSOD is a compilation of daily meteorological data produced by the National Climatic Data Center, available from 1929 to present, which displays a reasonably dense spatial coverage across Africa. However, a general caveat with the GSOD dataset is the limit imposed by its sparse gauge network. There are many regions, especially across Central Africa where the absence of temperature records precludes a comprehensive and robust analysis. To circumvent this limitation, daily reanalysis data have also been used. Reanalysis is a combination of observations and climatological models

through data assimilation systems to produce a single, uniform global dataset (Kalnay et al., 1996), thus enabling a homogeneous coverage of Africa.

The magnitude of heat waves for both observations and reanalysis is quantified on annual basis by means of the Heat Wave Magnitude Index daily (HWMId; Russo et al., 2015) for the period 1981–2015 across Africa. The HWMId has been applied to maximum and minimum temperature.

The objective of this paper is to analyse African heat wave regime and identify the most important of heat waves during 1981–2015. These analyses draw attention to the spatial distribution of temperature extremes and their temporal evolution in the past decades, still largely unknown. Considering both its wide geographic scope and spatial resolution, the study represents an important step towards the assessment of heat wave frequency in the last 3 decades using records of daily maximum and minimum temperatures acquired at regional level.

The availability of such information is paramount. The more reliable the assessment of heat waves is, the better African countries will be equipped to strengthen their coping capacities. This study also provides insight in human exposure to heat waves in Africa.

Some early exploratory research using similar methodology for South America showed some promising preliminary results (Ceccherini et al., 2016). In this paper, the heat wave classification scheme has been consolidated and improved (Russo et al., 2015) and both observations and reanalysis datasets have been employed.

2 Data and methodology

2.1 Data

The time series of temperature used in this study have been derived from (1) observations and (2) reanalysis. GSOD is the dataset of observations. GSOD records, produced by the National Climatic Data Center, are mainly recorded at international airports and include maximum and minimum values of temperature. GSOD records underwent extensive automated quality controls to eliminate many of the random errors found in the original data (further details on the GSOD data can be obtained from the website http://www.climate.gov/global-summary-day-gsod). GSOD has been already employed to assess heat waves magnitude at global (Mishra et al., 2015) and local (Ceccherini et al., 2016) scale. Historical data are generally available for the last 80 years, with data from 1973 onwards being the most complete. The total number of GSOD stations available across Africa is equal to 958. However, only 260 of them satisfy the conditions needed to calculate heat wave magnitude indices, as further described in the Methodology section.

ERA-Interim (Berrisford et al., 2011; Dee et al., 2011) is the dataset of reanalysis providing hydrometeorological variables such as maximum and minimum temperature, evaporation, snowfall, runoff and precipitation across land at various temporal scales. Reanalysis has been increasingly used to address a variety of climate-change issues and has by now become an important method in climate-change research (Fan and van den Dool, 2004; Marshall and Harangozo, 2000; Uppala et al., 2005). ERA-Interim is a reanalysis product of the European Centre for Medium-Range Weather Forecasts (ECMWF) available from 1979 and continuously updated in real time. The data assimilation system used to produce ERA-Interim is based on a 4-D variational scheme (4D-Var) with a 12 h analysis window (for further information on 4D-VAR see Courtier et al., 1994).

The reanalysis dataset used in this study has a spatial resolution of 0.75° (i.e. approximately 80 km at the equator) and a temporal resolution of 1 day (i.e. a time step of 24 h). The variables of interest are daily maximum and minimum temperature, ranging from 1981 to 2015. ERA-Interim allows a consistent spatial and temporal resolution over 3 decades, incorporating millions of observations into a stable data assimilation system. However, observational constraints, and therefore reanalysis reliability, can considerably vary depending on the location, time period and variable considered, thus introducing spurious variability and trends.

For both observations and reanalysis dataset the timespan considered in this study refers to the period 1 January 1981–30 June 2015.

2.2 Methodology

In this paper the HWMId, recently defined by Russo et al. (2015), has been employed to detect African heat waves for the period 1981–2015. The HWMId is a simple numerical indicator that takes both the duration and the intensity of the heat wave into account. Basically, the magnitude index sums excess temperatures beyond a certain normalized threshold and merges durations and temperature anomalies of intense heat wave events into a single indicator, according to the methodology described in Russo et al. (2014, 2015). The HWMId is an improvement on the previous Heat Wave Magnitude Index (i.e. HWMI by Russo et al., 2014) and able to overcome its limitations. More precisely, HWMI has some problems in assigning magnitude to very high temperatures in a changing climate, thus resulting in an underestimation of extreme events.

The HWMId is defined as the maximum magnitude of the heat waves in a year. Specifically, a heat wave is defined as a period ≥ 3 consecutive days with maximum temperature above a daily threshold calculated for a 30-year-long reference period. The threshold is defined as the 90th percentile of daily maxima temperature, centred on a 31-day window.

The interquartile range (IQR, i.e. the difference between the 25th and 75th percentiles of the daily maxima tempera-

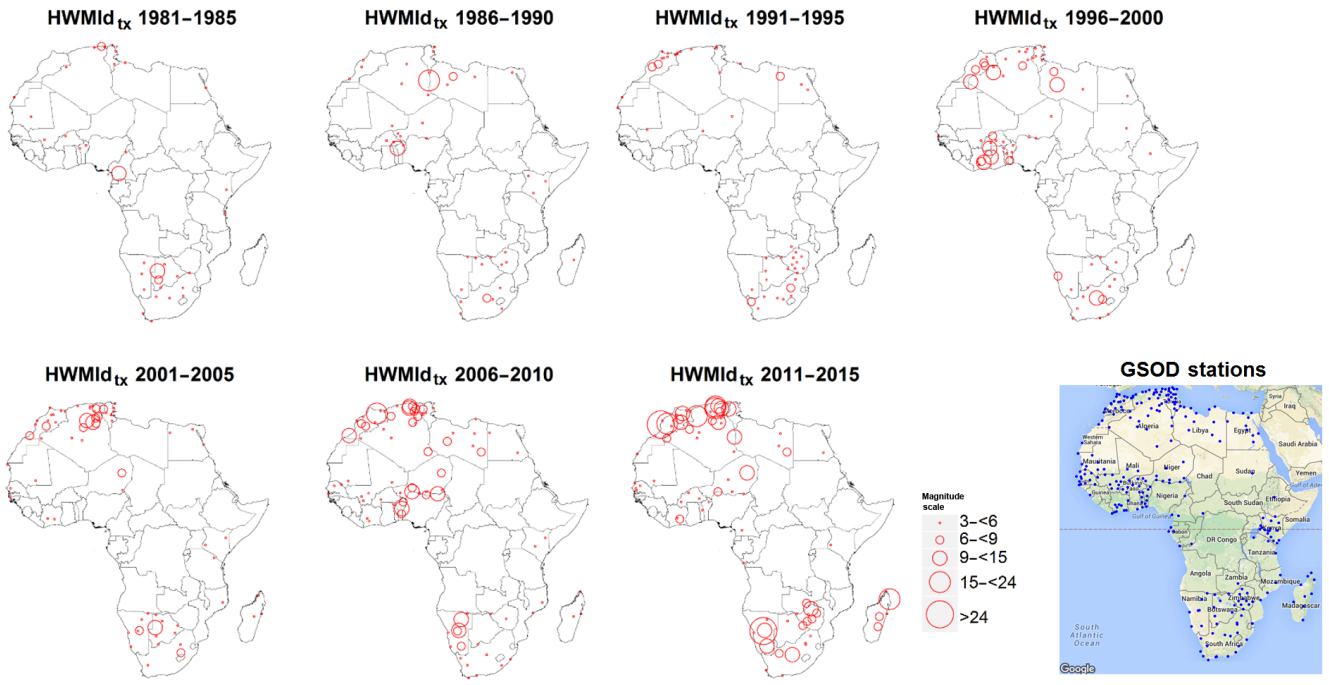

Figure 1. Heat Wave Magnitude Index daily of maximum temperature ($HWMId_{tx}$) for 5-year periods of GSOD records from 1981 to 2015. The bottom-right panes show the spatial distribution of the GSOD station employed in this study.

ture) is used as the heat wave magnitude unit, since it represents a non-parametric measure of the variability. If a day of a heat wave has a temperature value equal to IQR, its corresponding magnitude value will be equal to 1. According to this definition, if the magnitude on the day d is 3, it means that the temperature anomaly on the day d is 3 times the IQR. The HWMId has been already used to evaluate future impacts of heat waves in Africa until 2100 under different representative concentration pathways scenarios (Russo et al., 2016).

The HWMId computations requires at least a 30-year time series of daily temperature records. GSOD stations with less than 30-year records and with more than 30 % of gaps have been excluded from our analysis (for further details see Ceccherini et al., 2016). As a result, 260 GSOD stations out of 958 satisfy these conditions.

Heat waves are computed using (1) maximum (hereafter $HWMId_{tx}$) and (2) minimum (hereafter $HWMId_{tn}$) daily temperature, giving thus complementary information, respectively, on warm day and night conditions. HWMId has been computed on annual basis

1. for each GSOD station and
2. for the entire spatial domain of the daily ERA-Interim maxima and minima temperatures dataset across Africa. Specifically, the index has been computed separately for each cell at ~ 80 km spatial resolution.

Heat waves generally occur between December and January in the Southern Hemisphere and between June and July in the Northern. In order to avoid splitting event occurrences that happen within a regular calendar year, starting and ending dates have been redefined accordingly. Therefore, the HWMId computation starts on 1 January 1981 and ends on 31 December 2014 in the Northern Hemisphere. Similarly, the HWMId computation starts on 1 July 1981 and ends on 30 June 2015 in the Southern Hemisphere (for further information see HWMId function in Gilleland and Katz, 2011). Note that this scheme leaves the tropics out of consideration. Also, the southern hemispheric 6-month time shift causes temporal inconsistency in the dataset: the time span is 34 years in the Southern Hemisphere and 35 in the Northern. However, starting our analysis from 1980 would have further reduced the number of available GSOD stations from 260 to ~ 220, thus exaggerating the already patchy spatial distribution of the observational network.

3 Results

Figures 1 and 2 display the maximum value in 5-year periods of the HWMId of GSOD observations from 1981 to 2015 for maximum and minimum temperature, respectively. The bottom-right panel of Fig. 1 shows the spatial distribution of the 260 GSOD temperature stations employed in this study.

There is a clear indication that both intensity and spatial distribution of heat waves of maximum temperature are

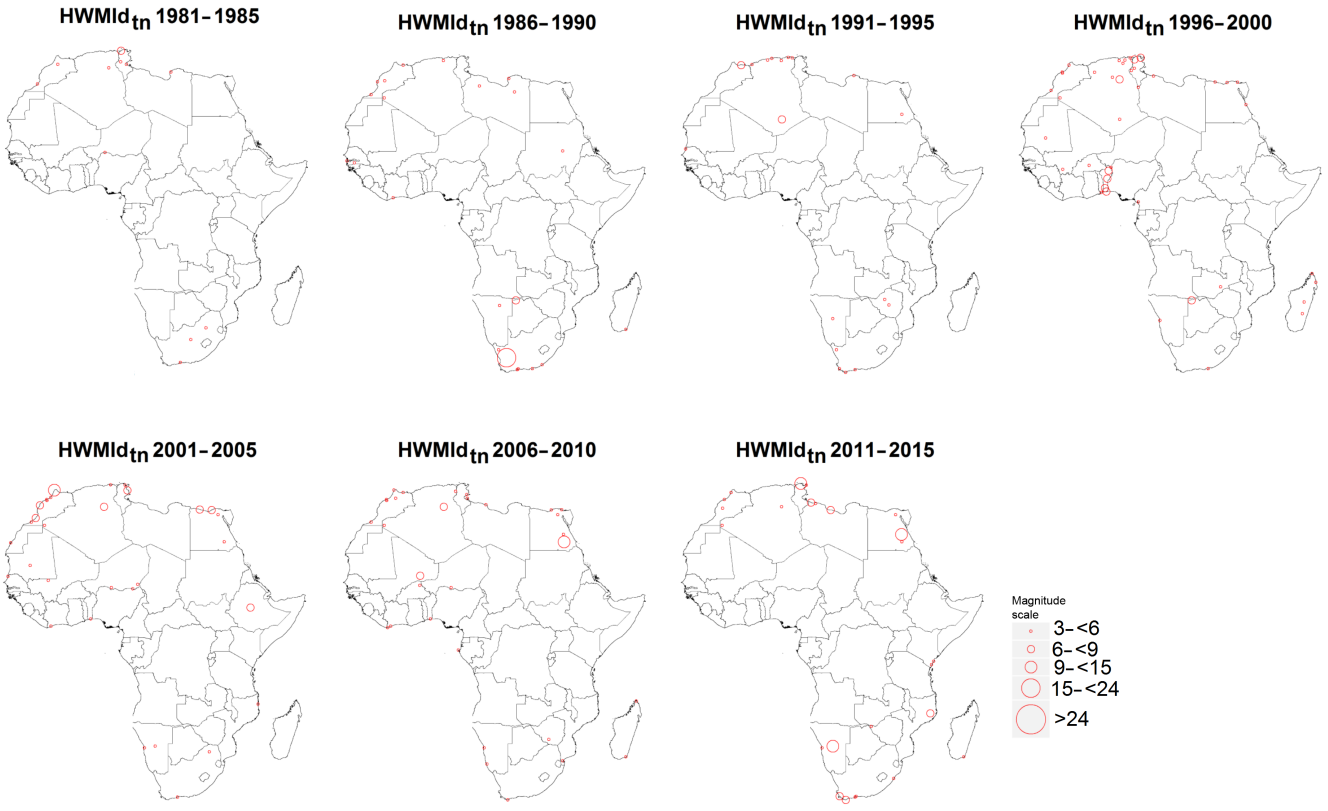

Figure 2. As Fig. 1 but applied to minimum temperature (HWMId$_{tn}$).

increasing. Specifically, from 1996 onwards it is possible to observe a positive increase in heat waves' magnitude and spread across Africa, with the maximum presence during 2011–2015. HWMId$_{tx}$'s frequency is below 40 events per 5-year period until 1995, and it then increases (histograms of heat waves for three classes of magnitude level are shown in Fig. S1 of the Supplement). Such increase of heat wave frequency corresponds with the findings of Fontaine et al. (2013): the occurrence of heat waves has clearly increased after 1996.

Despite the generally high correlation between maximum and minimum temperature, HWMId results with minimum temperature differ significantly from those with maximum temperature. Specifically, the number of stations affected by heat wave events of minimum temperature is low , i.e. ~ 10 events in the period 1981–1985 and ~ 40 events in the period 2011–2015 all over Africa. Figure 1 also shows that the temporal increase of heat wave events is not monotonic for all regions, e.g. in Sahel, which displays an intermittent behaviour rather than a monotonic growth.

The interannual evolution of heat waves is fully detailed in Fig. 3, which shows the occurrence of HWMId greater than a given magnitude level (i.e. HWMId ≥ 3, 6, 9, 15) for maximum and minimum temperature, respectively. Frequently reoccurring heat events are captured on these plots. Results confirm previous findings of Figs. 1 and 2. For maximum temperature the linear regression of occurrence of heat waves is statistically significant ($\alpha = 0.01$) for HWMId greater than 3, 6 and 9. Interestingly, the slope is reduced by half every step. Conversely, for minimum temperature it is possible to observe a statistical significant upwards trend only for heat waves with magnitude level greater than 3. Besides, minimum temperature exhibits a lower value of the slope and number of occurrences thereof.

As for GSOD, Fig. 4 shows the HWMId$_{tx}$ of the reanalysis dataset for 5-year periods from 1981 to 2015. Each pixel of the map represents the highest HWMId over the 5-year period. On the one hand, the 5-year temporal aggregation simplifies the visualization; on the other hand, it hinders the detection of frequently reoccurring events. However, these event occurring at annual scale are shown in Fig. S3. In the case of ERA-Interim, instead of counting the number of occurrences, we have estimated the spatial extent of heat waves as the land area fraction exceeding a fixed HWMId value. The area fraction is expressed in percentage. Reanalysis spatial coverage throughout Africa is continuous, circumventing thus the limitations of GSOD, where the locations of the observing stations might lead to a difference between the increases in occurrences in all of African versus observations made at these specific stations. The major limitation of the

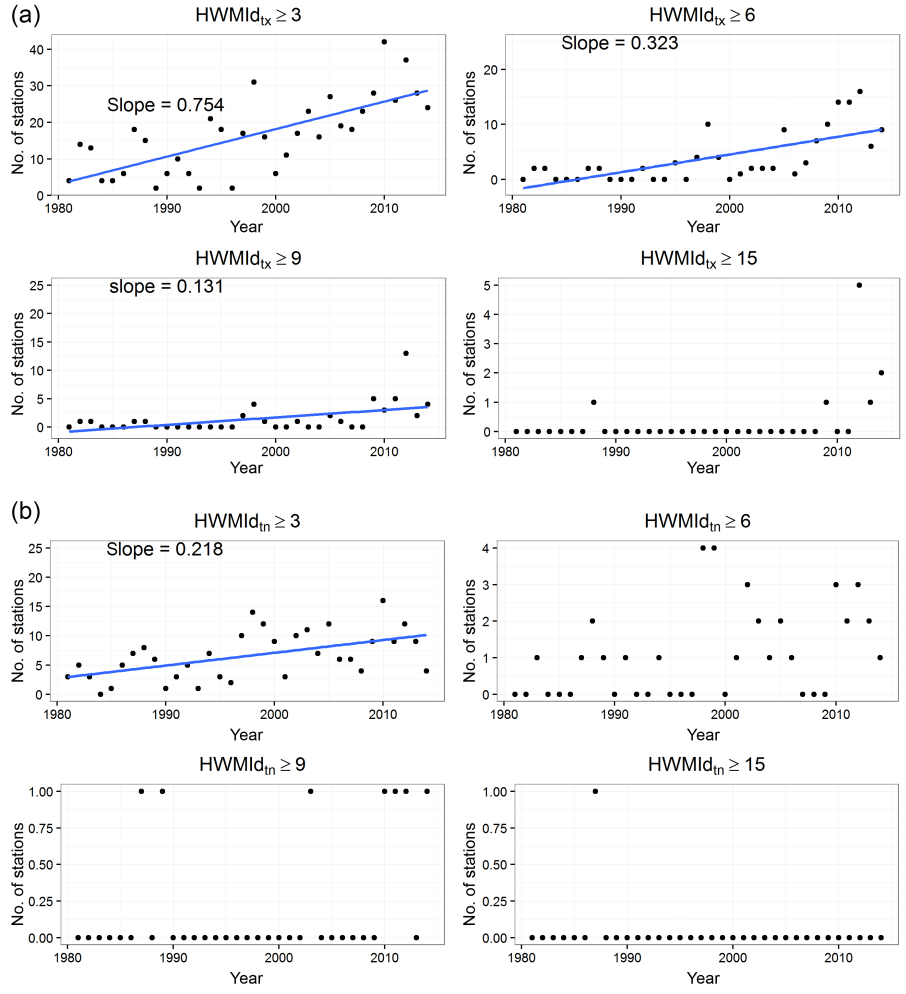

Figure 3. Annual distribution of events exceeding four different thresholds (i.e. HWMId ≥ 3, 6, 9, 15) for maximum (top panel) and minimum (bottom panel) temperature. The blue line represents the statistically significant ($\alpha = 0.01$) linear regression.

reanalysis is that uncertainties are difficult to understand and quantify (Simmons et al., 2010).

Spatial patterns indicate an increase of HWMId$_{tx}$ during the last 20 years. The major hot spot of increases in HWMId frequency and magnitude are located in northern Africa, ranging from Morocco to Egypt, and in Angola, Congo, South Sudan, Kenya and Madagascar.

Unlike our finds for GSOD, the temporal evolution of HWMId$_{tn}$ – shown in Fig. 5 – do not differ significantly from HWMId$_{tx}$. It is possible to distinguish an increase of heat wave intensity. This is noticeable from the analysis of the histograms in Fig. S2, where the maximum value of the percentage of land where heat waves occurred rises from ∼ 25 to ∼ 60 % per 5-year period.

Also, HWMId$_{tn}$ exhibits different spatial patterns; generally it occurs – with less intensity – in the same zone hit by maximum temperatures, but it also affects other zones. This increase in HWMId$_{tn}$ is noticeable across Angola, Congo, Zambia, Namibia and Botswana, while it is not present in northern Africa.

Just as for GSOD, Fig. 6 shows the occurrence of HWMId greater than a given magnitude level for maximum and minimum temperature, respectively. Maximum temperature displays a positive and statistically significant trend for the first three classes. The slopes of the linear regression are comparable with those of GSOD observations.

Unlike GSOD, the percentage of area affected by heat waves increase also for minimum temperature, which exhibits slopes comparable with those of maximum temperature even if they are slightly lower.

A visual comparison of heat wave detection from observations (GSOD) and reanalysis (ERA-Interim) is given in the Fig. S3. The maps show the HWMId$_{tx}$ as detected by GSOD network (blue circles) and ERA-Interim (gridded maps). For 1988, there is a good match between GSOD and reanalysis results across northern Africa. In addition, 1998 heat waves across western Africa and Morocco are well captured

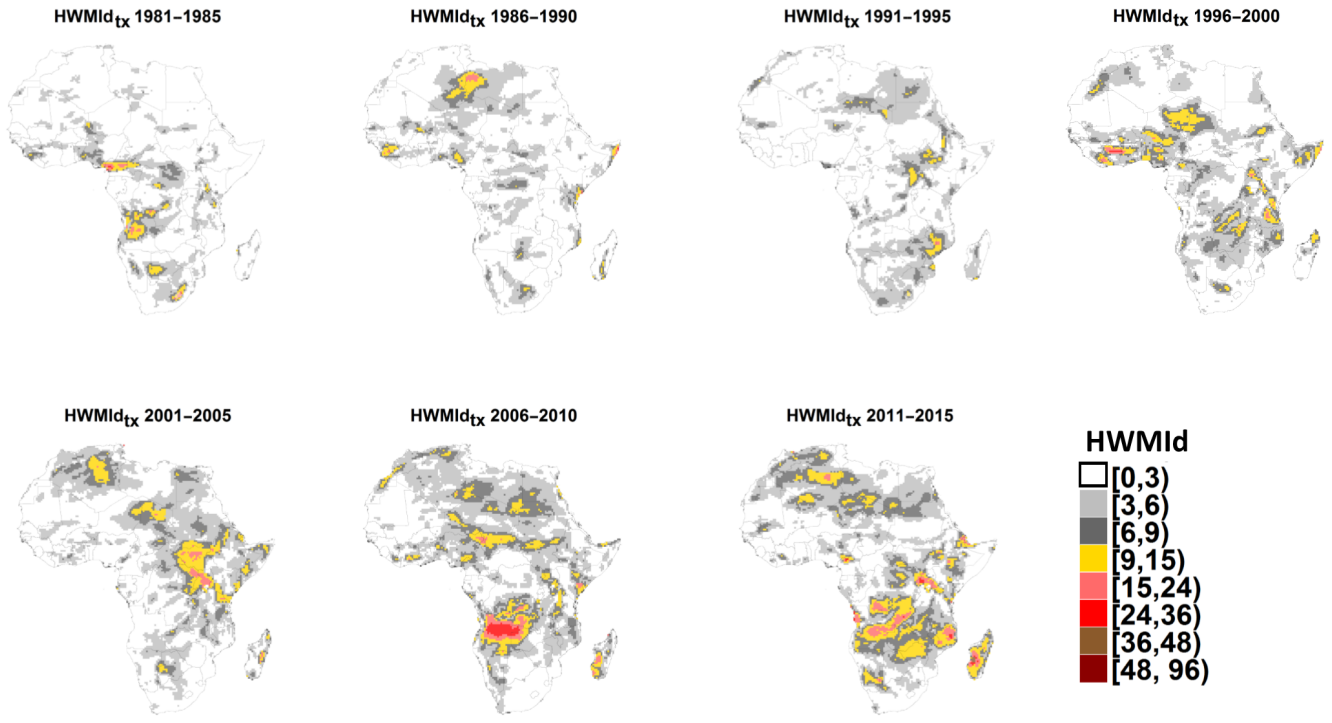

Figure 4. Heat Wave Magnitude Index daily of maximum temperature (HWMId$_{tx}$) for 5-year periods of ERA-Interim dataset from 1981 to 2015.

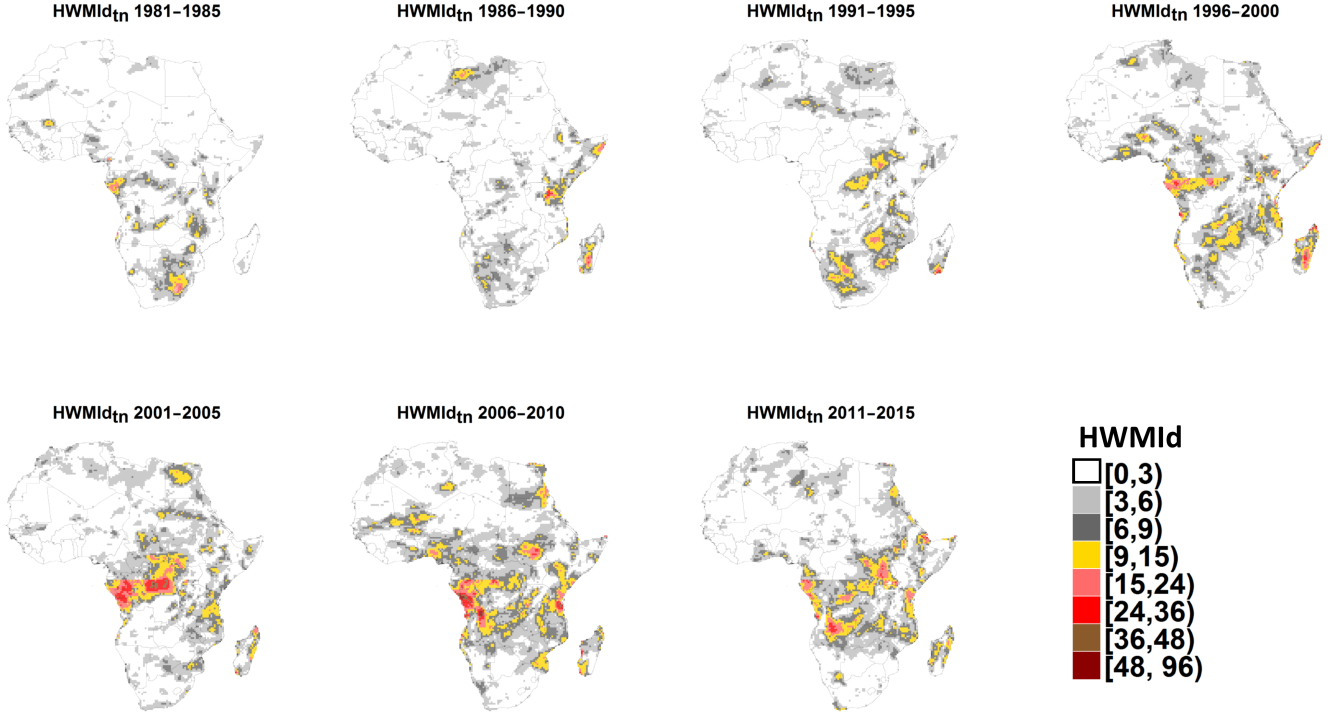

Figure 5. As Fig. 4 but applied to minimum temperature (HWMId$_{tn}$).

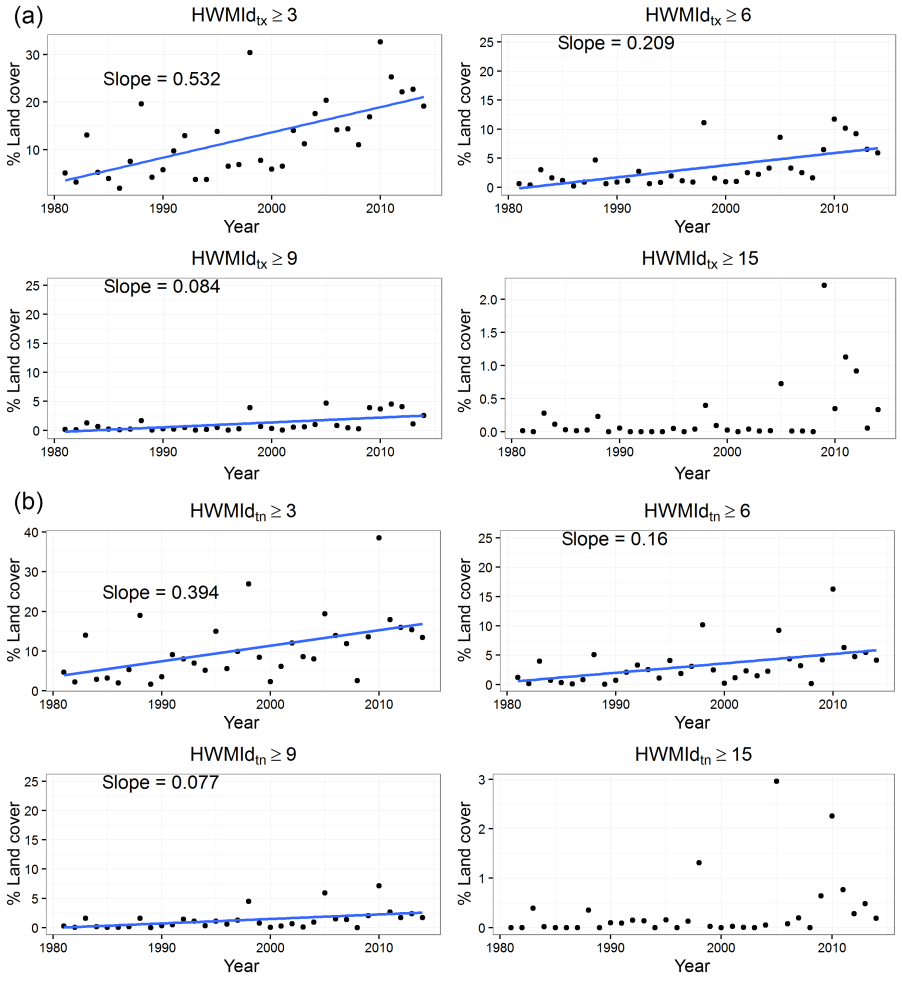

Figure 6. Annual distribution of events exceeding four different thresholds (i.e. HWMId ≥ 3, 6, 9, 15) for maximum (top panel) and minimum (bottom panel) temperature. Since the reanalysis-based HWMId is a gridded product, plots show the percentage of land area affected by heat waves rather than the number of events.

by both datasets. In regard to 2005, there is a good match throughout northern Africa. The 2012 heat wave events in Morocco and Algeria from GSOD are consistent with the reanalysis. Interestingly, this heat wave is well documented in both newspapers and literature (e.g. Blunden and Arndt, 2013). It is possible to observe consistency also during 2014 across Madagascar, Zimbabwe and northern Africa.

Although the qualitative character of the comparison due to the low GSOD station number, ERA-Interim shows good agreement with observations.

Although quantitative comparison between observation and reanalysis is crucial, it is as fraught with difficulties as it is necessary. Even when GSOD observations are available, they are limited to a few points in space and time that may not represent a ∼ 80 km reanalysis pixel. Besides, the spatial scales and resolutions of space-based and field instruments are so different that comparing the values generated by both approaches is difficult at best.

A quantitative comparison has been carried out by computing the confusion matrix of heat wave detection from observation and reanalysis. Tables 1 and 2 show the confusion matrices for the entire period 1981–2015 for maximum and minimum temperature, respectively. Heat waves have been classified into four classes, i.e. HWMId ≤ 1, 1 < HWMId ≤ 3, 3 < HWMId ≤ 6 and HWMId > 6. For the sake of simplicity we omitted those events not classified as heat waves (i.e. HWMId ≤ 1) by both observation and reanalysis.

The vast majority of the elements of the matrices are not on the top-left to bottom-right diagonal, i.e. the correct classification. Besides, we can observe a "decay" of the number of events correctly classified when the magnitude level increases. This is also due to the lower number of intense heat waves compared to the moderate ones.

The off-diagonal elements represent classification errors, i.e. the number of heat waves that ended up in another class

Table 1. Confusion matrix of heat wave detection from observation (GSOD) and reanalysis (ERA-Interim) for maximum temperature for the period 1981–2015.

		ERA-Interim			
		HWMId ≤ 1	$1 <$ HWMId ≤ 3	$3 <$ HWMId ≤ 6	HWMId > 6
GSOD	HWMId ≤ 1	–	501	143	40
	$1 <$ HWMId ≤ 3	894	172	53	17
	$3 <$ HWMId ≤ 6	321	101	30	15
	HWMId > 6	149	42	19	10
	Sensitivity	0.69	0.21	0.12	0.12

Table 2. Confusion matrix of heat wave detection from observation (GSOD) and reanalysis (ERA-Interim) for minimum temperature for the period 1981–2015.

		ERA-Interim			
		HWMId ≤ 1	$1 <$ HWMId ≤ 3	$3 <$ HWMId ≤ 6	HWMId > 6
GSOD	HWMId ≤ 1	–	344	61	10
	$1 <$ HWMId ≤ 3	920	117	31	4
	$3 <$ HWMId ≤ 6	357	58	12	5
	HWMId > 6	177	36	10	2
	Sensitivity	0.70	0.21	0.11	0.10

during GSOD and ERA-Interim classification. For both maximum and minimum temperature we can observe that ERA-Interim often underestimates GSOD-based heat waves.

Overall, the values of accuracy of classification for maximum and minimum temperature are 0.58 and 0.64, respectively. Note that these values are highly influenced by the correct detection of HWMId ≤ 1 which represent the vast majority of the events. The sensitivity, i.e. an indicator of the performance of the classifier, indicates that HWMId ≤ 3 are easier to be detected than higher classes by both databases. The scatterplots of observations versus reanalysis are shown in Fig. S4.

Figure 7 shows the density plot of population affected by heat waves of maximum temperature (HWMId_{tx}) detected by reanalysis in 2011. Population count refers to the LandScan database (Bright et al., 2012) and it has been resampled to the ERA-Interim cell size, i.e. $0.75° \times 0.75°$. Note that the cell area of the gridded ERA-Interim product varies depending on the longitude. As expected, low-intensity heat waves (i.e. HWMId ≤ 3) are more frequent across highly populated areas, but interestingly the highest events (i.e. HWMId ≥ 9, on the right of the black vertical line) might affect the vast majority of African population.

2011 results indicate that heat waves generally occur on populated areas. Similar results, shown in Fig. S5, using another population count dataset, namely the Joint Research Centre Urban Settlement Layer (Freire and Pesaresi, 2016), are obtained for 2014. The Joint Research Centre Urban Settlement Layer has been used to test another population dataset and further highlight this specific risk. The fact that two different years present similar patterns highlights the vulnerability of the African region and the importance of heat wave assessment and prediction.

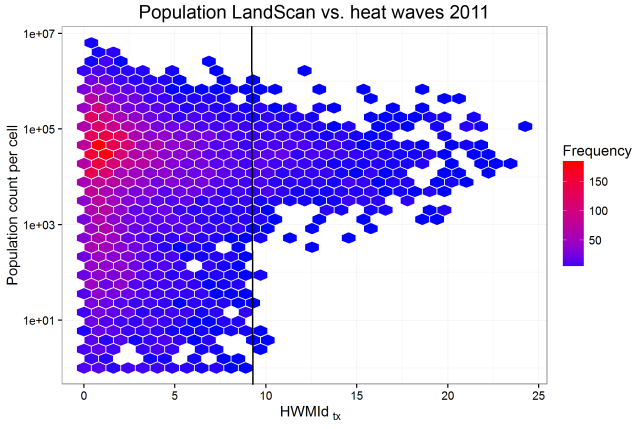

Figure 7. Density plot of population affected by heat waves of maximum temperature detected by reanalysis in 2011 using the LandScan population count database. The y axis refers to the population count per cell, where the cell is the $0.75° \times 0.75°$ ERA-Interim pixel. The black vertical line is at HWMId $= 9$.

4 Conclusions

In this work we present the results of the application of the HWMId in the assessment of climate change across Africa. Observation from GSOD and reanalysis from ERA-Interim datasets are used to identify heat waves, their temporal and spatial variability and their impacts on African population. GSOD observations are able to capture heat wave events at fine spatial scales, but they show a sparse coverage across Africa. Conversely, the reanalysis dataset, despite the coarse spatial resolution and the uncertainties, displays a homogeneous coverage.

Results from maximum temperature (HWMId_{tx}) indicate an increase in intensity and frequency of extreme events using both observation and reanalysis.

Specifically, from 1996 onwards it is possible to observe HWMId_{tx} spread with the maximum presence during 2006–2015.

Between 2006 and 2015 the frequency (spatial coverage) of extreme heat waves had increased to 24.5 observations per year (*60.1 % of land cover*), as compared to 12.3 per year (37.3 % of land area) in the period from 1981 to 2005 for GSOD stations (reanalysis). Both observation and reanalysis show a positive trend of stations/land area experiencing HWMId values greater than magnitude level equal to 3, 6 and 9. The slopes of linear regressions decrease with increasing of magnitude levels.

Minimum temperature exhibits incoherence between the results of GSOD and ERA-Interim. GSOD-based HWMId_{tn} shows a positive trend only for stations experiencing HWMId values greater than 3. Conversely, the reanalysis-based HWMId_{tn} shows a dramatic increase in extreme events. This rise, albeit minor, is comparable with that pertaining to maximum temperature. Besides, there is spatial coherence between maximum and minimum temperature from reanalysis, even when heat waves of minimum temperature also occurred in other regions.

The pertinence of ERA-Interim HWMId is evaluated through comparisons with GSOD records, recognizing that point measurements on the ground may not adequately represent the hydrometeorological variability generally present in the reanalysis pixel. Our results also show coherence between observation-based and reanalysis-based heat waves using a visual comparison. Instead, the quantitative analysis indicates that heat waves with a high (i.e. HWMId > 3) magnitude level are difficult to be detected at the same time by both databases. However, a correct comparison is fraught with difficulties and could be possible only with very dense (and well-established) meteorological networks, such as those in Europe or the US.

Many events are well documented in the news, indicating that HWMId is able to capture events that are perceived as heat waves by a broader public. Finally, the analysis of population hit by heat waves shows that the highest events affect the most populated regions rather than the uninhabited ones.

Our work has direct relevance for both scientists and policy makers. Increasing numbers of heat waves may pose challenges on health care and on electric supply for residential cooling demands, among others. These implications argue for the importance of enhancing the density of hydrometeorological stations to provide the baseline data that will be essential (1) for climate-change adaptation and (2) to reduce the uncertainties of reanalysis products. Further applications include (1) the employment of HWMId scheme to climatological models to quantify the increase in heat wave for the next decades; (2) the wider and quantitative implications of African heat waves on health, crops and finance; and (3) the analysis of teleconnections between the 2015/2016 El Niño event (Cesare, 2015) and heat waves in eastern Africa.

5 Data availability

Dataset can be accessible from (1) Global Summary of the Day (GSOD) version 8, National Climatic Data Center (ftp://ftp.ncdc.noaa.gov/pub/data/gsod/), and (2) ERA-Interim, produced daily by the European Centre for Medium-Range Weather Forecasts (ECMWF)(http://apps.ecmwf.int/datasets/data/interim-full-daily).

The Supplement related to this article is available online at doi:10.5194/nhess-17-115-2017-supplement.

Competing interests. The authors declare that they have no conflict of interest.

Acknowledgements. Authors would like to thank the valuable support from JRC. This work has received funding from European Commission EuropeAid Co-operation Office under the grant agreement RALCEA. The data used in this paper can be obtained from (1) Global Summary of the Day (GSOD) version 8, National Climatic Data Center (ftp://ftp.ncdc.noaa.gov/pub/data/gsod/); and (2) ERA-Interim, produced daily by the European Centre for Medium-Range Weather Forecasts (ECMWF) (http://apps.ecmwf.int/datasets/data/interim-full-daily). The authors also thank those responsible for the efforts on providing free tools such as R used in this work. The R packages were obtained from the Comprehensive R Archive Network (http://cran.r-project.org/) or R-forge (https://r-forge.r-project.org/). Heat Wave Magnitude Index daily has been calculated using the R library "extRemes" (Gilleland, 2015). Google data are registered trademarks of Google Inc., used with permission. Population analysis was made by utilizing the LandScan (2011, 2012)^{TM} High Resolution Global Population Data Set copyrighted by UT-Battelle, LLC, operator of Oak Ridge National Laboratory under contract no. DE-AC05-00OR22725 with the US Department of Energy. Maps are available upon request. The authors acknowledge Hugh Eva for his help editing the paper.

Edited by: V. Kotroni
Reviewed by: D. Lee and two anonymous referees

References

Albrecht, T.: http://documents.worldbank.org/curated/en/2014/11/20404287/turn-down-heat-confronting-new-climate-normal-vol-2-2-main-report or http://www-wds.worldbank.org/external/default/WDSContentServer/WDSP/IB/2014/11/20/000406484_20141120090713/Rendered/PDF/927040v20WP00O0ull0Report000English.pdf (last access: January 2017), 2014.

Berrisford, P., Dee, D. P., Poli, P., Brugge, R., Fielding, K., Fuentes, M., Kållberg, P. W., Kobayashi, S., Uppala, S., and Simmons, A.: The ERA-Interim archive Version 2.0, ECMWF, Shinfield Park, Reading, 2011.

Blunden, J. and Arndt, D. S.: State of the Climate in 2012, B. Am. Meteorol. Soc., 94, S1–S258, doi:10.1175/2013BAMSStateoftheClimate.1, 2013.

Bright, E. A., Coleman, P. R., Rose, A. N., and Urban, M. L.: LandScan 2011, available at: http://www.ornl.gov/landscan/ (last access: 16 May 2016), 2012.

Ceccherini, G., Russo, S., Ameztoy, I., Romero, C. P., and Carmona-Moreno, C.: Magnitude and frequency of heat and cold waves in recent decades: the case of South America, Nat. Hazards Earth Syst. Sci., 16, 821–831, doi:10.5194/nhess-16-821-2016, 2016.

Cesare, C.: Developing El Niño could be strongest on record, Nature, doi:10.1038/nature.2015.18184, in press, 2015.

Collins, J. M.: Temperature Variability over Africa, J. Climate, 24, 3649–3666, doi:10.1175/2011JCLI3753.1, 2011.

Courtier, P., Thépaut, J.-N., and Hollingsworth, A.: A strategy for operational implementation of 4D-Var, using an incremental approach, Q. J. Roy. Meteorol. Soc., 120, 1367–1387, doi:10.1002/qj.49712051912, 1994.

Dee, D. P., Uppala, S. M., Simmons, A. J., Berrisford, P., Poli, P., Kobayashi, S., Andrae, U., Balmaseda, M. A., Balsamo, G., Bauer, P., Bechtold, P., Beljaars, A. C. M., van de Berg, L., Bidlot, J., Bormann, N., Delsol, C., Dragani, R., Fuentes, M., Geer, A. J., Haimberger, L., Healy, S. B., Hersbach, H., Hólm, E. V., Isaksen, L., Kållberg, P., Köhler, M., Matricardi, M., McNally, A. P., Monge-Sanz, B. M., Morcrette, J.-J., Park, B.-K., Peubey, C., de Rosnay, P., Tavolato, C., Thépaut, J.-N., and Vitart, F.: The ERA-Interim reanalysis: configuration and performance of the data assimilation system, Q. J. Roy. Meteorol. Soc., 137, 553–597, doi:10.1002/qj.828, 2011.

Fan, Y. and van den Dool, H.: Climate Prediction Center global monthly soil moisture data set at 0.5° resolution for 1948 to present, J. Geophys. Res.-Atmos., 109, D10102, doi:10.1029/2003JD004345, 2004.

Fontaine, B., Janicot, S., and Monerie, P.-A.: Recent changes in air temperature, heat waves occurrences, and atmospheric circulation in Northern Africa, J. Geophys. Res.-Atmos., 118, 8536–8552, doi:10.1002/jgrd.50667, 2013.

Freire, S. and Pesaresi, M.: GHS population grid, derived from GPW4, multitemporal (1975, 1990, 2000, 2015) – CKAN, available at: http://data.jrc.ec.europa.eu/dataset/jrc-ghsl-ghs_pop_gpw4_globe_r2015a, last access: 2 December 2016.

Gilleland, E.: extRemes: Extreme Value Analysis, available at: https://cran.r-project.org/web/packages/extRemes/index.html last access: 9 September 2015.

Gilleland, E. and Katz, R. W.: New Software to Analyze How Extremes Change Over Time, Eos T. Am. Geophys. Un., 92, 13–14, doi:10.1029/2011EO020001, 2011.

Kalnay, E., Kanamitsu, M., Kistler, R., Collins, W., Deaven, D., Gandin, L., Iredell, M., Saha, S., White, G., Woollen, J., Zhu, Y., Leetmaa, A., Reynolds, R., Chelliah, M., Ebisuzaki, W., Higgins, W., Janowiak, J., Mo, K. C., Ropelewski, C., Wang, J., Jenne, R., and Joseph, D.: The NCEP/NCAR 40-Year Reanalysis Project, B. Am. Meteorol. Soc., 77, 437–471, doi:10.1175/1520-0477(1996)077<0437:TNYRP>2.0.CO;2, 1996.

Marshall, G. J. and Harangozo, S. A.: An appraisal of NCEP/NCAR reanalysis MSLP data viability for climate studies in the South Pacific, Geophys. Res. Lett., 27, 3057–3060, doi:10.1029/2000GL011363, 2000.

Mishra, V., Ganguly, A. R., Nijssen, B., and Lettenmaier, D. P.: Changes in observed climate extremes in global urban areas, Environ. Res. Lett., 10, 024005, doi:10.1088/1748-9326/10/2/024005, 2015.

Russo, S., Dosio, A., Graversen, R. G., Sillmann, J., Carrao, H., Dunbar, M. B., Singleton, A., Montagna, P., Barbola, P., and Vogt, J. V.: Magnitude of extreme heat waves in present climate and their projection in a warming world, J. Geophys. Res.-Atmos., 119, 12500–12512, doi:10.1002/2014JD022098, 2014.

Russo, S., Sillmann, J., and Fischer, E. M.: Top ten European heatwaves since 1950 and their occurrence in the coming decades, Environ. Res. Lett., 10, 124003, doi:10.1088/1748-9326/10/12/124003, 2015.

Russo, S., Marchese, A. F., Sillmann, J., and Immé, G.: When will unusual heat waves become normal in a warming Africa?, Environ. Res. Lett., 11, 054016, doi:10.1088/1748-9326/11/5/054016, 2016.

Simmons, A. J., Willett, K. M., Jones, P. D., Thorne, P. W., and Dee, D. P.: Low-frequency variations in surface atmospheric humidity, temperature, and precipitation: Inferences from reanalyses and monthly gridded observational data sets, J. Geophys. Res.-Atmos., 115, D01110, doi:10.1029/2009JD012442, 2010.

Solomon, S., Intergovernmental Panel on Climate Change, Intergovernmental Panel on Climate Change and Working Group I: Climate change 2007: the physical science basis: contribution of Working Group I to the Fourth Assessment Report of the Intergovernmental Panel on Climate Change, Cambridge University Press, Cambridge, UK, 2007.

UNECA: Assessment of Africa's Climatic Records and Recording Networks Including Strategic for Rescuing of Climatic Data, UNECA, available at: http://www1.uneca.org/acpc/acpcworkingpapers.aspx (last access: 5 January 2016), 2011.

Uppala, S. M., KÅllberg, P. W., Simmons, A. J., Andrae, U., Bechtold, V. D. C., Fiorino, M., Gibson, J. K., Haseler, J., Hernandez, A., Kelly, G. A., Li, X., Onogi, K., Saarinen, S., Sokka, N., Allan, R. P., Andersson, E., Arpe, K., Balmaseda, M. A., Beljaars, A. C. M., Berg, L. V. D., Bidlot, J., Bormann, N., Caires, S., Chevallier, F., Dethof, A., Dragosavac, M., Fisher, M., Fuentes, M., Hagemann, S., Hólm, E., Hoskins, B. J., Isaksen, L., Janssen, P. a. E. M., Jenne, R., Mcnally, A. P., Mahfouf, J.-F., Morcrette, J.-J.,

Rayner, N. A., Saunders, R. W., Simon, P., Sterl, A., Trenberth, K. E., Untch, A., Vasiljevic, D., Viterbo, P., and Woollen, J.: The ERA-40 re-analysis, Q. J. Roy. Meteorol. Soc., 131, 2961–3012, doi:10.1256/qj.04.176, 2005.

WMO: WMO five-year analysis, available at: https://www.wmo.int/media/content/wmo-2015, last access: 30 November 2015.